

UNCLASSIFIED

AD NUMBER

AD821751

LIMITATION CHANGES

TO:

Approved for public release; distribution is unlimited.

FROM:

Distribution: Further dissemination only as directed by Army Electronics Command, ATTN: AMSEL-KL-TG, Fort Monmouth, NJ 07703-5601, SEP 1967, or higher DoD authority.

AUTHORITY

USASC ltr dtd 16 Jun 1971

THIS PAGE IS UNCLASSIFIED

RESEARCH AND DEVELOPMENT TECHNICAL REPORT  
ECOM — 01821-6

INVESTIGATION OF HIGH-POWER  
BEAM PLASMA INTERACTIONS

6th QUARTERLY REPORT

By

*CLAUDE LUSTIG*

*PHILIP STONE*

*HARRY EWALD*

SEPTEMBER 1967

DISTRIBUTION STATEMENT

Each transmittal of this document outside  
the Department of Defense must have prior  
approval of CG, Army Electronics  
Command, Fort Monmouth, N.J.  
Attn: AMSEL-RL-TG

OCT 30 1967

A

ECOM

UNITED STATES ARMY ELECTRONICS COMMAND • FORT MONMOUTH, N.J. 07703  
Sponsored By Advanced Research Projects Agency Under Project Defender

CONTRACT DA 28-043-AMC-01821(E), ARPA Order No. 695

SPERRY RAND RESEARCH CENTER

Sperry Rand Corporation  
Sudbury, Massachusetts 01776

**BEST  
AVAILABLE COPY**

## **N O T I C E S**

### **DISPOSITION**

**Destroy this report when it is no longer needed. Do not return it to the originator.**

### **DISCLAIMERS**

**The citation of trade names and names of manufacturers in this report is not to be construed as official Government indorsement or approval of commercial products or services referenced herein.**

**The findings in this report are not to be construed as an official Department of the Army position, unless so designated by other authorized documents.**

INVESTIGATIONS OF HIGH-POWER  
BEAM PLASMA INTERACTIONS

6th QUARTERLY REPORT  
15 March 1967 - 14 June 1967

Report No. 6  
Contract No. DA 28-043-AMC-01821(E)  
DA Project No. 7900.21.243.40.01

Prepared By  
Claude Lustig, Philip Stone and Harry Ewald  
Sperry Rand Research Center

for  
U. S. Army Electronics Command, Fort Monmouth, N. J. 07703

Sponsored By  
Advanced Research Projects Agency  
ARPA Order No. 695

This research is part of PROJECT DEFENDER, sponsored by the Advanced Research Projects Agency, Department of Defense, and administered by the U. S. Army Electronics Command, under Contract No. DA 28-043-AMC-01821(E).

DISTRIBUTION STATEMENT

This document may be further distributed by any holder only with specific prior approval of CG, U. S. Army Electronics Command, Fort Monmouth, N. J. Attn: AMSEL-KL-TG

SPERRY RAND RESEARCH CENTER  
Sperry Rand Corporation  
Sudbury, Massachusetts 01776

## ABSTRACT

This research is directed toward the investigation of high-power beam plasma interactions, with specific investigation of the transverse velocity beam modes called for.

The dispersion relation for electrostatic waves propagating at an oblique angle to the magnetic field has been calculated. Strong damping occurs unless the axial wavelength is at least one or two orders of magnitude greater than the perpendicular wavelength. In experiments with the modulated-beam apparatus, we have found that the electrostatic waves are excited more strongly as the transverse energy of the beam is increased. Experiments are being carried out to obtain a quantitative measure of the transverse energy of an electron beam.

This research is part of PROJECT DEFENDER, sponsored by the Advanced Research Project Agency, Department of Defense, and administered by the U. S. Army Electronics Command under Contract No. DA 28-043-AMC-01821(E).

# TABLE OF CONTENTS

<u>Section</u>	<u>Page</u>
I      PURPOSE	1
II     INTRODUCTION AND STATEMENT OF PROBLEM	1
III    TECHNICAL BACKGROUND	2
A. Linear Theory of Waves in a Uniform Plasma or Beam	2
B. The Effect of Gradients	7
IV     WORK PERFORMED DURING REPORT PERIOD	17
A. Theoretical	17
B. Modulated-Beam Experiment	18
1. Beam Excitation of Longitudinal Waves	18
2. Axial Measurements	22
C. Two-Beam Experiment	22
V      CONCLUSIONS	27
VI     FUTURE PLANS	27
LITERATURE CITED	28

# LIST OF ILLUSTRATIONS

<u>Figure</u>		<u>Page</u>
1	Dispersion diagram of so-called electron beam where electrons move only along the magnetic field with a single speed (in this case zero velocity).	4
2	Dispersion diagram for transverse beam modes on a mono-energetic beam of spiraling electrons.	5
3	Dispersion relation for mono-energetic, fixed perpendicular energy beam waves of frequency less than the first cyclotron harmonic.	8
4	Growth rate and frequency of growing waves associated with the interaction of the positive energy beam wave with the negative energy beam wave on the same beam as a function of the ratio of cyclotron to beam plasma frequency.	9
5	Reactive interaction between a transverse velocity beam and a warm plasma.	10
6	Electric potential associated with the radial wave resonances on a plasma column.	13
7	Experimentally observed radial electron plasma wave resonances in the core of a cylindrical plasma column for different magnetic field strengths.	15
8	Experimental apparatus showing method of excitation as well as method of internal probing of radial resonances on a plasma column in magnetic field.	16
9	The real part of $\sqrt{\lambda_{\perp}}$ vs $\omega/\Omega$ for a range of $\lambda_{\parallel}$ . The Bernstein modes are $\lambda_{\parallel} = 0$ . The curves for $\lambda_{\parallel} > 0$ eventually bend into the origin. The dots are experimental points (see Sec. B).	19
10	The imaginary part of $\sqrt{\lambda_{\perp}}$ vs $\omega/\Omega$ for a range of $\lambda_{\parallel}$ . The Bernstein modes are $\lambda_{\parallel} = 0$ and have zero imaginary part (no damping). The $I_m/\lambda_{\perp}$ must be $< 0.01$ for reasonable damping.	20
11	The intensity of the probe signal as a function of its radial position without magnetic-field modulation or phase-sensitive detection.	21



# LIST OF ILLUSTRATIONS (cont.)

<u>Figure</u>		<u>Page</u>
12	The intensity of the signal at the first and third radial peaks as a function of corkscrew current.	23
13	The intensity of the signal (same units as in Fig. 12) at the second and fourth radial peaks as a function of corkscrew current.	23
14	Phase variation of the signal with the antenna fixed as a function of beam voltage for two magnetic fields.	24
15	Experimental setup for measuring the azimuthal flux on an electron beam with a probe with two exposed surfaces.	26
16	Differential probe output as a function of helix current.	26

## I. PURPOSE

This investigation has as its purpose the theoretical and experimental investigation of new (i.e., not space charge) modes of beam plasma interaction. In particular, it includes the investigation of the feasibility of these new modes as an improved means of generation and amplification of microwaves.

## II. INTRODUCTION AND STATEMENT OF PROBLEM

It is apparent from recent developments in the linear theory of plasma waves (of which electron beam waves are a subgroup) that the wave interactions used thus far in devices for microwave generation and amplification represent only a small fraction of those which are possible and which should be considered. Performance and design limitations of existing devices are due to the characteristics of the particular waves used, and they may well be extended or removed if different waves are employed.

The Sperry Rand Research Center (SRRC) has contracted to conduct a comprehensive theoretical and experimental study of particular plasma waves (including electron beam waves) which are candidates for application to high-power microwave generators or amplifiers, and which have not as yet been adequately investigated.

The work being undertaken is an extension of research which has been in progress at SRRC. As a result of company sponsored investigations performed during the past three years, an important set of beam and plasma waves - the so-called electrostatic, cyclotron-harmonic waves - have been identified. These waves merit further study because they remove the plasma density, magnetic field, and parallel phase velocity restrictions inherent in the wave modes used in existing devices. Their dispersion relation has been formulated and solved for many interesting cases, including growing wave interactions.

In particular the research program includes: measurement of propagation characteristics for comparison with existing linear dispersion theory; coordinated theoretical and experimental study of the effect of finite geometry, velocity spread, and density and temperature gradients on linear propagation characteristics and wave impedance; a primarily experimental study of non-linear amplitude limiting and spurious frequency generation; and a study of the noise properties of the amplification medium. Special emphasis will be given to a search for practical methods of efficiently coupling these waves to conventional transmission lines.

The program will also include extension of the range of solutions to linear plasma and beam wave dispersion relations in a search for additional wave modes of potential usefulness in high-power microwave devices. For while the past theoretical program at SRRC has been extensive, there remain many possible relative orientations of beam velocity, wave velocity, rf electric field and dc magnetic field vectors, wide ranges of parameters, and many beam and plasma velocity distributions of potential interest which have not yet been considered.

### III. TECHNICAL BACKGROUND

#### A. LINEAR THEORY OF WAVES IN A UNIFORM PLASMA OR BEAM

The non-relativistic dispersion relation for high-frequency electrostatic waves in an infinite uniform electron medium neutralized by massive ions is:

$$\frac{\omega_p^2}{k_\perp^2 + k_\parallel^2} \sum_{n=-\infty}^{\infty} \int_0^\infty v_\perp dv_\perp \int_{-\infty}^{\infty} dv_\parallel \frac{2\pi J_n^2(k_\perp v_\perp / \Omega)}{\omega - k_\parallel v_\parallel - n\Omega} \left( \frac{n\Omega}{v_\perp} \frac{\partial}{\partial v_\perp} + k_\parallel \frac{\partial}{\partial v_\parallel} \right) f_0(v_\perp, v_\parallel) = -1 \quad (1)$$

where

$$\omega_p^2 = \frac{ne^2}{\epsilon_0 m}$$

$k_\parallel$  = component of propagation vector along the static magnetic field,  $B_0$ .

$k_\perp$  = component of propagation vector across the static magnetic field.

$f_0(v_\perp, v_\parallel)$  = the normalized electron velocity distribution, where  $v_\perp$  is the velocity across the field and  $v_\parallel$  is the velocity along the field.

$$\Omega = \frac{eB_0}{m}$$

and  $J_n(k_\perp v_\perp / \Omega)$  is the Bessel function of the first kind and order  $n$  with argument  $k_\perp v_\perp / \Omega$ .

The importance of the distribution function in determining the behavior of the waves which may be supported in the medium is striking. To begin with, if we consider an electron beam with velocity parallel to the magnetic field, then

$$f_0(v_\perp, v_\parallel) = \frac{1}{2\pi v_\perp} \delta(v_\perp) \delta(v_\parallel - v_{0\parallel})$$

and the dispersion relation is

$$k_{\parallel}^2 \frac{\omega_p^2}{(\omega - k_{\parallel} v_{0\parallel})^2} + k_{\perp}^2 \frac{\omega_p^2}{(\omega - k_{\parallel} v_{0\parallel})^2 - \Omega^2} = k_{\perp}^2 + k_{\parallel}^2 \quad (2)$$

This equation, originally discussed by Gould and Trivelpiece,<sup>1</sup> describes the fast and slow space charge waves as well as the fast and slow fundamental cyclotron waves. The case of a finite beam diameter has also been discussed in detail.<sup>2</sup> The general conclusion drawn from the simple case of a uniform density finite diameter beam is that the geometry merely restricts the set of  $k$  values ( $k_{\perp}, k_{\parallel}$ ) which can be used to satisfy (2) but that the infinite medium dispersion equation must still be satisfied. The dispersion diagram for this "cold" electron beam is given in Fig. 1. It will be noted that the slow "negative energy" waves used for oscillators or amplifiers have a parallel phase velocity less than the beam velocity.

When electron motion about the lines of magnetic field is taken into account, an infinite set of waves is found.<sup>3,4</sup> In addition to modified space charge waves, two waves exist for each harmonic of the electron cyclotron frequency. One of each such pair of waves is found to have negative energy,<sup>5</sup> and can thus be used for growing wave interaction, as is the slow space charge wave in conventional microwave tubes. The dispersion curve shown in Fig. 2 is for a beam of monoenergetic, spiraling electrons, whose velocity distribution is given by

$$f_0(v_{\perp}, v_{\parallel}) = \frac{1}{2\pi v_{0\perp}} \delta(v_{\perp} - v_{0\perp}) \delta(v_{\parallel} - v_{0\parallel})$$

and whose dispersion relation is

$$k^2 = k_{\perp}^2 + k_{\parallel}^2 = \omega_p^2 \sum_{n=-\infty}^{\infty} \left[ \frac{k_{\parallel}^2 J_n^2(k_{\perp} v_{0\perp} / \Omega)}{(\omega - k_{\parallel} v_{0\parallel} - n\Omega)^2} + \frac{k_{\perp}^2 [J_{n-1}^2(k_{\perp} v_{0\perp} / \Omega) - J_{n+1}^2(k_{\perp} v_{0\perp} / \Omega)]}{2n(\omega - k_{\parallel} v_{0\parallel} - n\Omega)} \right] \quad (3)$$

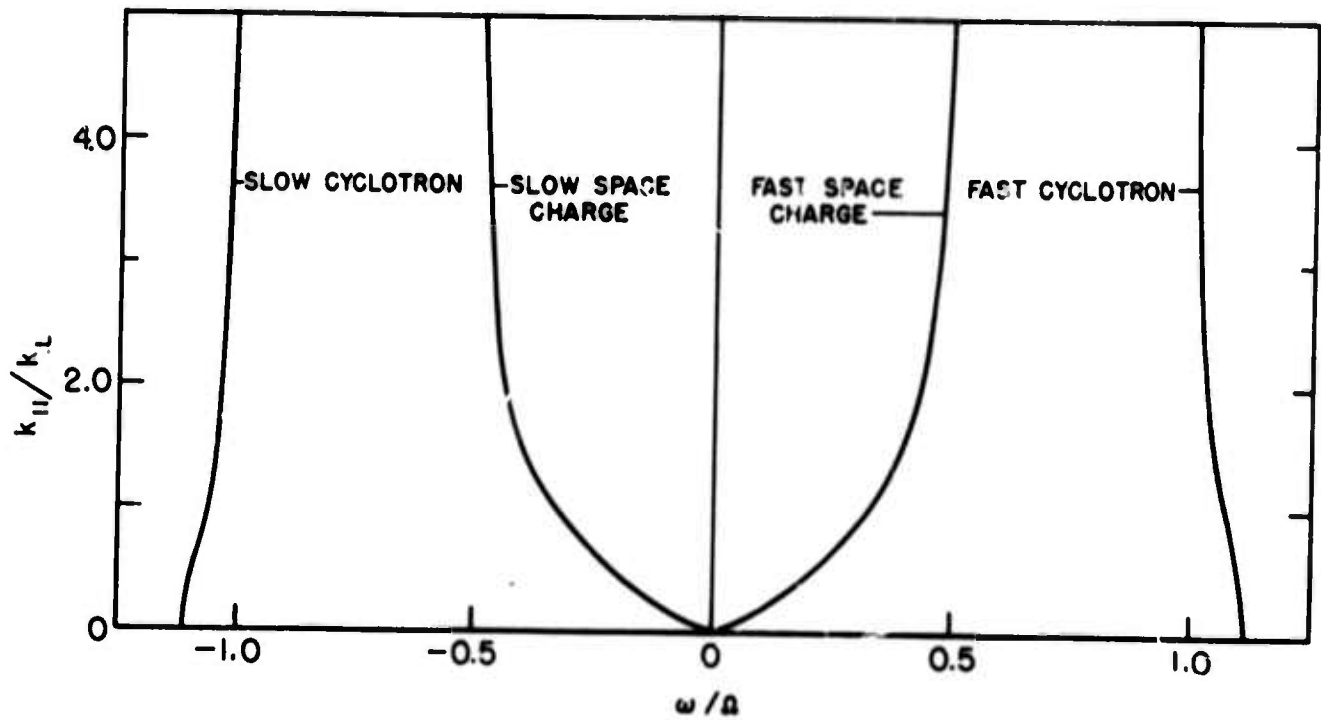


FIG. 1 Dispersion diagram of so-called cold electron beam where electrons move only along the magnetic field with a single speed (in this case zero velocity). The beam plasma frequency divided by the cyclotron frequency  $\omega_p/\Omega = 0.5$  for the example chosen.

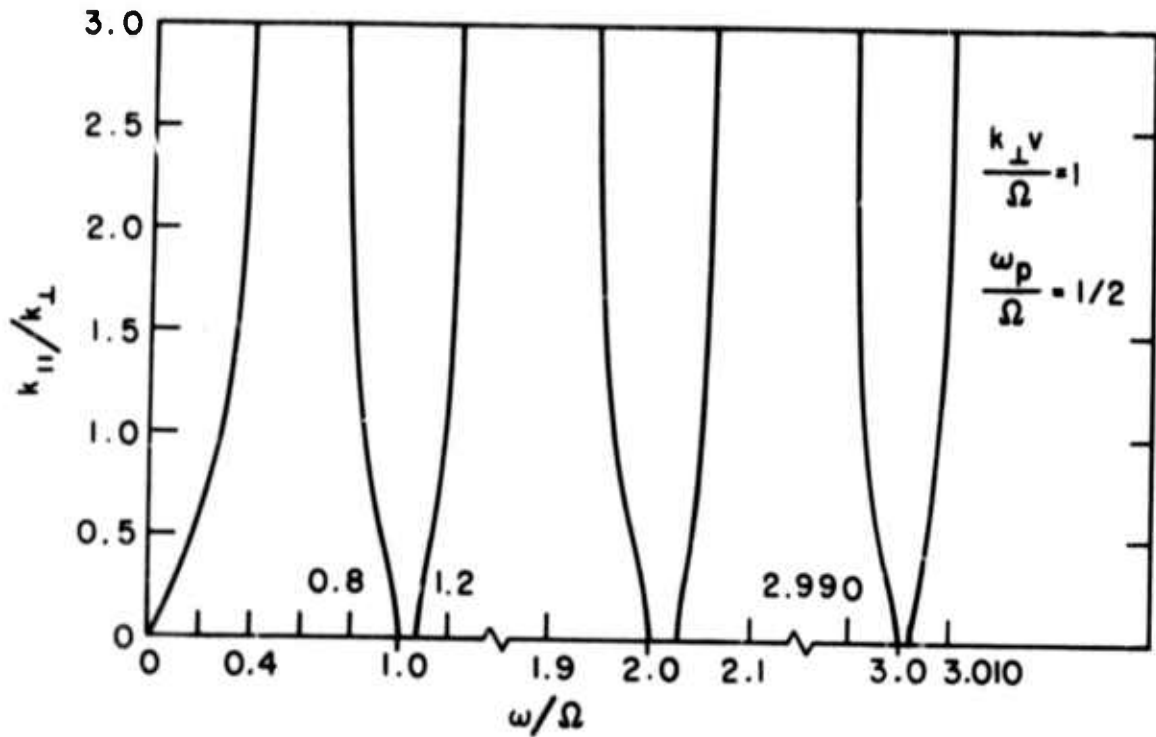


FIG. 2 Dispersion diagram for transverse beam modes on a mono-energetic beam of spiraling electrons. Only positive frequencies are shown for convenience. The dispersion relation is symmetric about both axes. Here again  $\omega_p/\Omega = 0.5$  but  $v_{0\perp} = \Omega/k_{\perp}$  (fixed  $k_{\perp}$ ).

If we consider an electron beam whose distribution function is Maxwellian across the field and having a single velocity along the field, then the results of using this in Eq. (1) yields

$$k^2 = k_{\perp}^2 + k_{\parallel}^2 = \omega_p^2 \sum_{n=-\infty}^{\infty} I_n(\lambda) e^{-\lambda} \left[ \frac{k_{\parallel}^2 v_{\perp}^2}{(\omega - k_{\parallel} v_{0\parallel} - n\Omega)^2} + \frac{n\Omega}{(\omega - k_{\parallel} v_{0\parallel} - n\Omega)} \right] \quad (4)$$

where

$$\lambda = (k_{\perp} v_{\perp} / \Omega)^2 .$$

Equation (3) exhibits certain interesting characteristics which in principle may be utilized in a power generation system. Consider the function in the last sum on the right-hand side of the equation,

$$J_{n-1}^2(\rho) - J_{n+1}^2(\rho) = J_n(\rho) \frac{d}{d\rho} J_n(\rho) .$$

where

$$\rho = k_{\perp} v_{0\perp} / \Omega .$$

This function becomes negative whenever  $J_n(\rho)$  and its derivative are of opposite sign. It is possible, for a sufficiently dense beam, to have instability over critical perpendicular velocity ranges for which  $J_n(\rho) d/d\rho J_n(\rho)$  is negative. Too much velocity spread in the perpendicular direction can eliminate these unstable regions, however, since the Maxwellian velocity distribution beam does not exhibit this characteristic. Our theoretical investigation will include detailed calculations of the effect both of perpendicular velocity spread (we will employ a shifted Maxwellian distribution with variable velocity spread) and of axial velocity spread, a spread which leads to the so-called "collisionless cyclotron damping."

Interaction between the transverse velocity, negative energy wave on the beam near the cyclotron harmonic and a circuit (or beam or plasma) positive energy wave leads to wave growth. This is dramatically illustrated in Fig. 3, where we present the negative and positive energy waves on a single electron beam. As the beam electron density increases, the positive energy wave originating at zero frequency for  $k_{\parallel} = 0$  (the fast space charge wave) couples with the negative-energy transverse velocity wave at the cyclotron frequency, and an instability results in growing wave solutions.<sup>6</sup> The growth rate and frequency spectrum of these waves are presented in Fig. 4 for several harmonics of the electron cyclotron frequency.

The interaction of a monoenergetic beam excited in the transverse velocity mode with a plasma whose electrons have a Maxwellian velocity distribution has been considered under somewhat restricted conditions by us. We have found wave growth in the region where the axially-traveling beam electrons see the cyclotron harmonic frequencies after the approximate doppler shift. This interaction occurs if the plasma appears to be lossy (resistive instability) or slightly reactive (reactive instability). In Fig. 5 we show the results of a calculation of the reactive instability.

The effect of boundaries in a finite beam of uniform electron density is subtly complicated by the non-zero orbits of the electrons. Those electrons traveling on field lines within a Larmor radius of the outer edge of the beam penetrate through the beam boundary and, hence, through what would be a region of radial field discontinuity. These electrons may interact more strongly with harmonics of the cyclotron motion than electrons nearer the axis.<sup>7</sup>

## B. THE EFFECT OF GRADIENTS

The importance of density and temperature gradients in beams or plasmas is well recognized. Because of theoretical difficulties, few attempts toward adequate solutions have been made. Recently, Nickel, Parker and Gould<sup>8</sup> and others investigated the effect of plasma gradients upon electrostatic waves propagating across a plasma column in order to explain the so-called Tonks-Dattner resonances which occur with no magnetic field. Buchsbaum and Hasegawa<sup>9</sup> and Schmitt, Meltz and Freyheit<sup>10</sup> have considered wave propagation across a radial density gradient in a magnetized plasma. In all cases, it is assumed that the change in density across a Larmor orbit is either so small that the gradient slightly perturbs the wave-equation or so large that the zero magnetic field condition is valid.

Emission<sup>11</sup> and absorption<sup>9,10</sup> measurements of a plasma column immersed in a magnetic field have shown very interesting fine structure when the frequency of observation is in the vicinity of twice the electron cyclotron frequency (and higher harmonics as well). The theory of Buchsbaum and Hasegawa is that waves can propagate within the high-density core of the plasma out toward the walls of the discharge tube until the wave frequency corresponds to the local hybrid frequency ( $\omega_{\text{hybrid}} = \sqrt{\omega_p^2 + \Omega_e^2}$ ), as long as the wave frequency is less than the second harmonic of the cyclotron frequency.



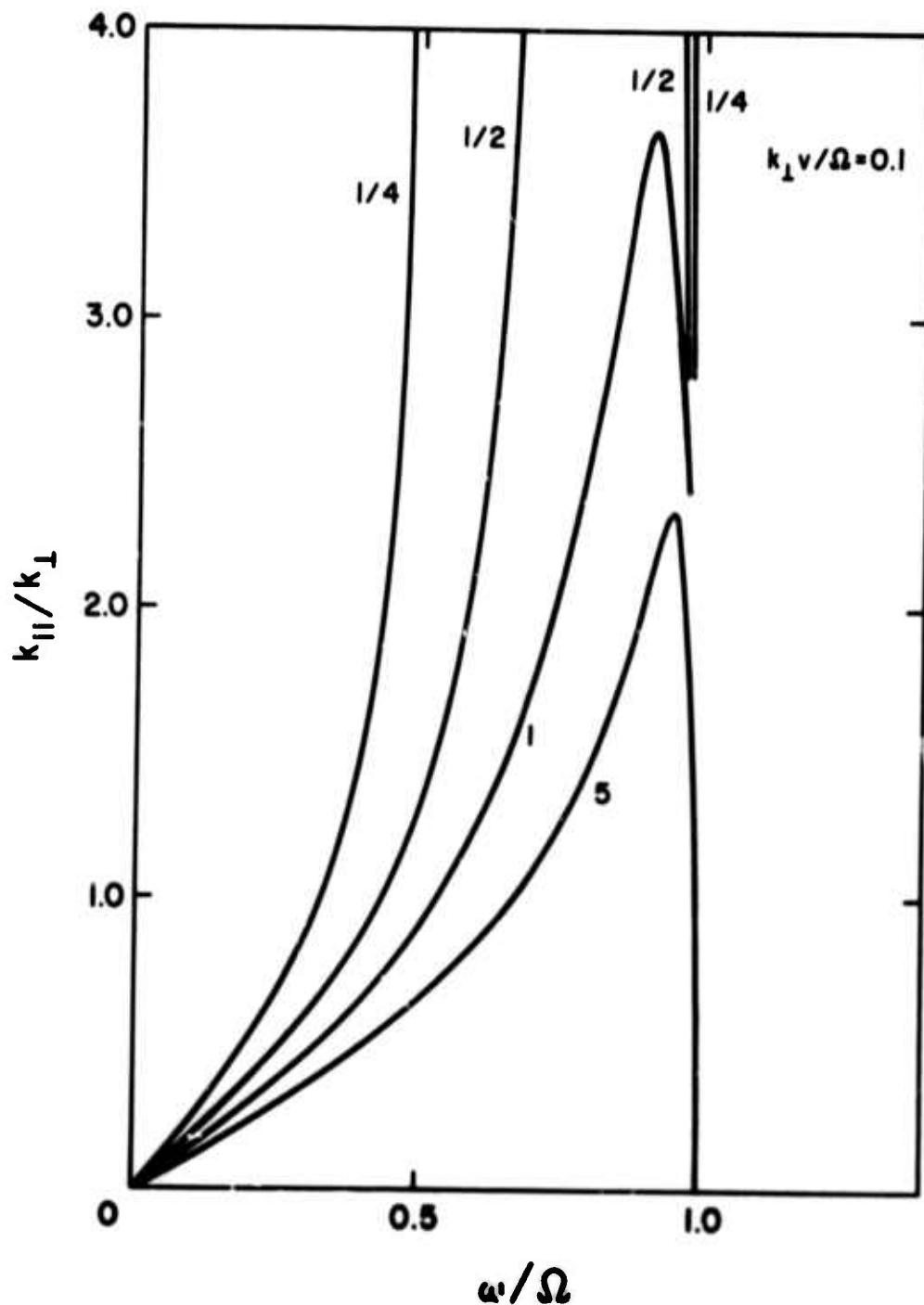


FIG. 3 Dispersion relation for mono-energetic, fixed perpendicular energy beam waves of frequency less than the first cyclotron harmonic. Each curve is for different beam density expressed in terms of the ratio  $\omega_p/\Omega$  all having  $k_{\perp} v_{0\perp} = 0.1\Omega$ . As density increases, the wave originating near zero frequency couples with the negative energy wave below the cyclotron frequency, and wave growth ensues.

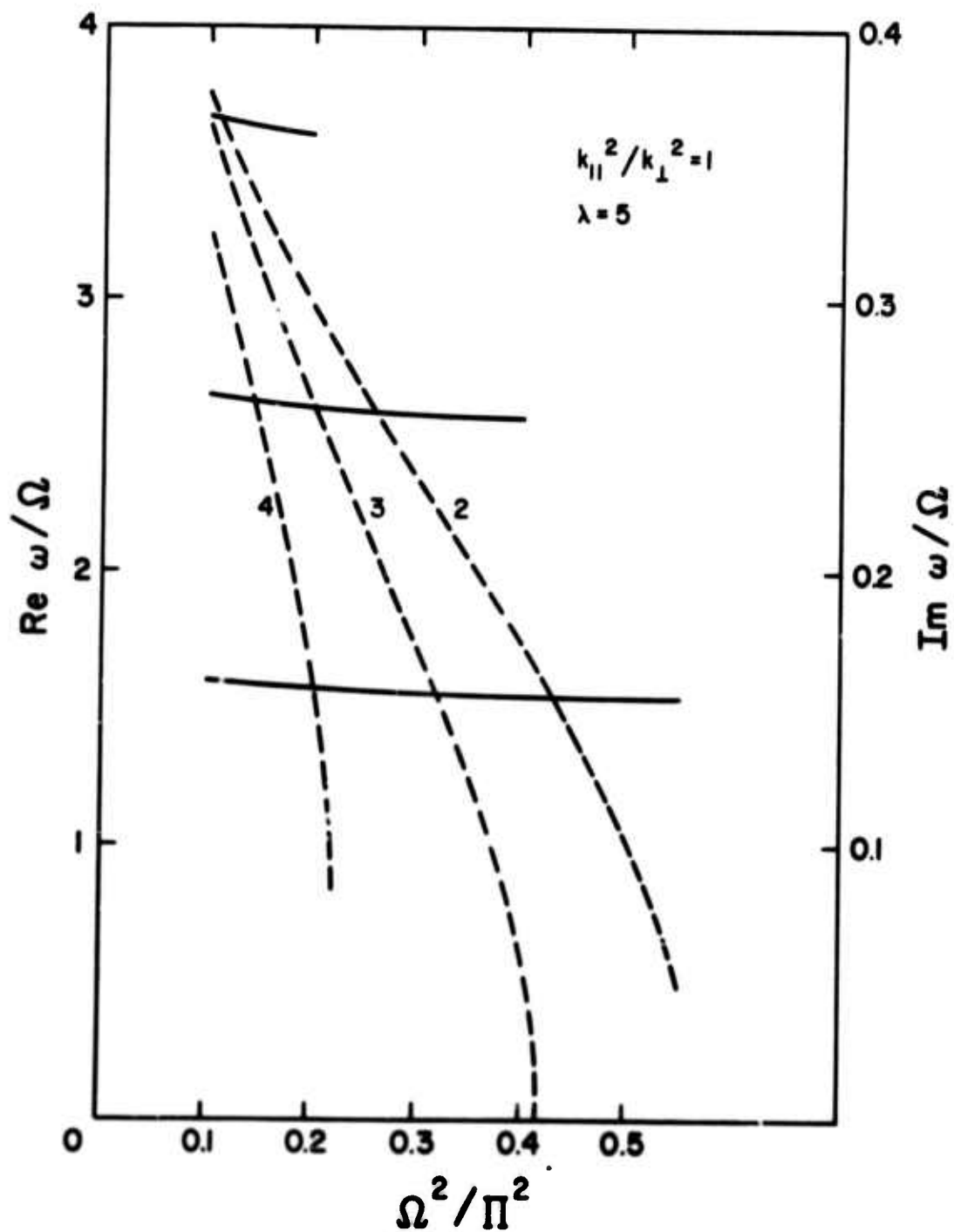


FIG. 4 Growth rate and frequency of growing waves associated with the interaction of the positive energy beam wave with the negative energy beam wave on the same beam as a function of the ratio of cyclotron to beam plasma frequency. Growth curves are shown by the dashed lines.

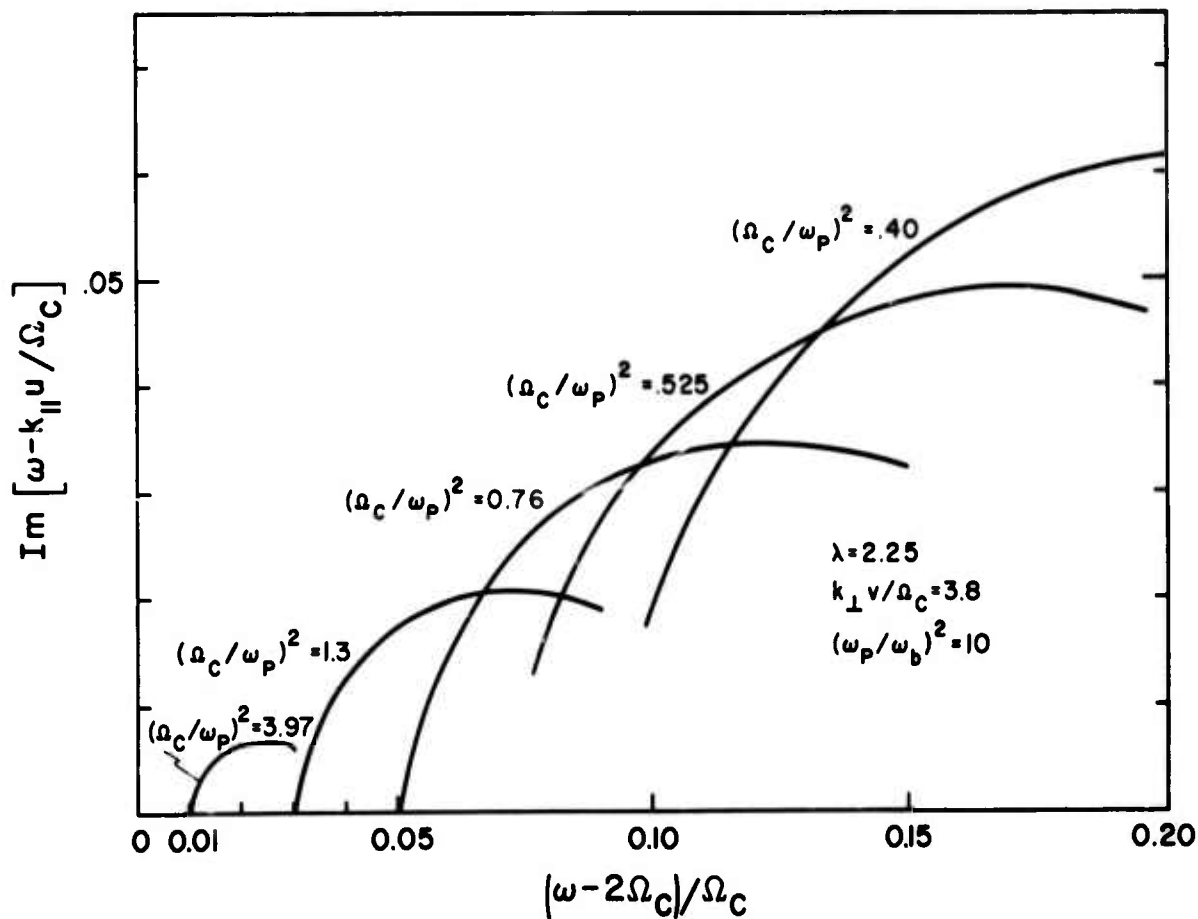


FIG. 5 Reactive interaction between a transverse velocity beam and a warm-plasma. Growth rate vs frequency is presented for waves near the second harmonic of the electron cyclotron frequency. Each curve represents a different plasma electron density, thus showing growth rate and frequency depend upon plasma frequency.

At the hybrid frequency the waves become evanescent on the outside and are reflected toward the interior, thus setting up a standing wave or radial resonant condition. The importance of radial density gradients is stressed by their analysis.

The combination of the linearized Boltzmann equation with Poisson's equation leads to the following differential equation for slab geometry:

$$\frac{d^2}{dx^2} [g(x)E(x)] + \frac{1}{\lambda^2} \left[ \frac{\omega_{po}^2}{\omega^2 - \Omega^2} - \frac{1}{g(x)} \right] g(x)E(x) = 0 \quad (5)$$

where

$$\lambda^2 = \frac{3eT/m \omega_{po}^2}{(\omega^2 - \Omega^2)(4\Omega^2 - \omega^2)} .$$

$T$  is the electron temperature (assumed to be uniform),  $g(x)$  is the normalized electron density profile, and  $\omega_{po}$  is the peak electron plasma frequency.

If the medium is uniform,  $g = 1$  and  $d^2/dx^2 \rightarrow -k^2$ , so that the dispersion relation is

$$(4\Omega^2 - \omega^2)(\Omega^2 + \omega_{po}^2 - \omega^2) = k_{\perp}^2 \left( \frac{3eT}{m} \right) \omega_{po}^2 \quad (6)$$

from which we can verify that

$k$  is real where  $\omega^2 < \Omega^2 + \omega_{po}^2$  and  $2\Omega > \omega$  .

$k$  is real where  $\omega^2 > \omega_{po}^2 + \Omega^2$  and  $2\Omega < \omega$  .

Case 2 has been experimentally and theoretically treated by Schmitt, Melitz and Freyheit.<sup>10</sup>

The solution of Eq. (5) can be explicitly given for a density profile

$$g(x) = \frac{1}{1 + \nu \left(\frac{x}{l}\right)^2}$$

and is

$$E(x) = \left[ 1 + \nu \left(\frac{x}{l}\right)^2 \right] \left[ D_{\nu/c} \left(\frac{x}{l}\right) \pm D_{\nu/c} \left(\frac{-x}{l}\right) \right]$$

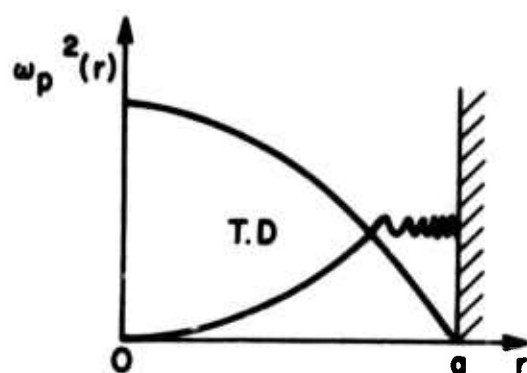
where

$$c = \left[ \frac{\frac{3eT}{m} \omega_{po}^2 l^2}{4\nu(\omega^2 - \Omega^2)(\Omega^2 - \omega^2)} \right]^{1/4}$$

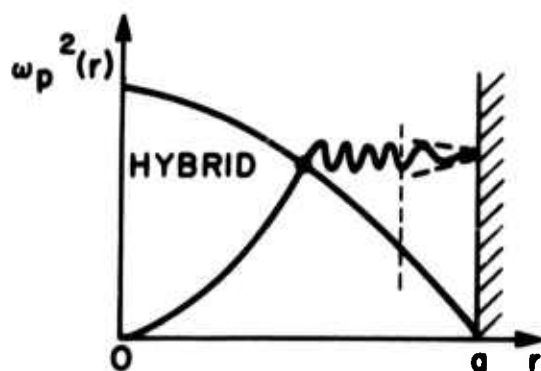
$$\nu = \frac{1}{2} \left[ \left\{ \frac{(\Omega^2 - \omega^2) l^2}{3\omega_{po}^2 \frac{eT}{m} (\omega^2 - \Omega^2)} \right\}^{1/2} (\Omega^2 + \omega_{po}^2 - \omega^2) - 1 \right]$$

and the  $D$  functions are parabolic cylinder functions. These functions oscillate in space in the manner of a radial standing wave, showing that physically the wave propagating out from the core is continuously reflected from the density gradient. Buchsbaum and Hasegawa's work has been extended by us to include cylindrical geometry, and the same essential feature of the standing wave pattern is found. In Fig. 6 we illustrate the nature of the solutions associated with waves propagating across a density gradient both with and without a static axial magnetic field.

The solution given above for the non-uniform plasma is valid only in the region where  $\omega \approx 2\Omega$  and is a result of an expansion to first order in the quantity  $(L_r d/dx)$ , which is the ratio of Larmor orbit  $(L_r^2 = eT/m\Omega^2)$  to gradient scale length. In order to consider waves in the

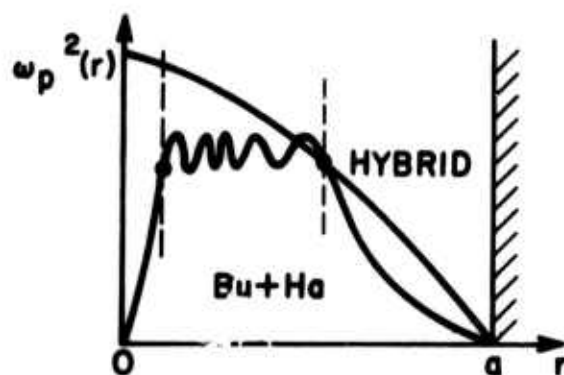


$$\Omega = 0$$



$$p < \frac{\epsilon}{\Omega} < p+1$$

$$(p \geq 2)$$



$$\frac{\epsilon}{\Omega} > 1$$

FIG. 6 Electric potential associated with the radial wave resonances on a plasma column. Three cases are indicated: Tonks-Dattner (TD) resonances with no magnetic field, the Buchsbaum-Hasegawa core resonances (B-H) in a magnetic field and external resonances in a magnetic field.

vicinity of the third harmonic, terms to second order in  $L_r d/dx$  are required and so on. It is obvious that computational complications increase with higher harmonic number if such a technique is used. We propose to consider the extension of this method as well as attempting different attacks on the problem.

While a plasma will probably have only slightly non-uniform electron temperature, an electron beam may well have a velocity distribution (it would be incorrect to consider it a temperature) which is highly inhomogeneous as a result of generation and injection methods. The terms arising from inhomogeneous beam electron velocity distribution (and density gradients) in the Boltzmann equation are from the term  $v_0 \nabla_r f_0$ , where  $f_0 = n(r)g_\perp(r, v_\perp)g_\parallel(r, v_\parallel)$ . That is, we assume that the density and velocity variations are separable. For example, we could consider a local Maxwellian velocity distribution in the  $\perp$  direction,

$$g_\perp(r, v_\perp) = \frac{1}{\sqrt{2\pi v_{\perp 0}^2(r)}} \exp\left(-\frac{v_\perp^2}{2v_{\perp 0}^2(r)}\right).$$

The consequences of such a distribution (or, for that matter, of any temperature gradient) upon the cyclotron harmonic beam waves are not evident, but approaching the problem via a perturbation technique allows the insights obtained in the uniform analysis to be extended and applied to the very difficult case of spatial temperature variation. That is, we can consider

$$v_{\perp 0}^2(r) = v_{\perp 0}^2 \left[ 1 + \gamma \left(\frac{r}{\ell}\right)^2 \right]$$

where  $\gamma$  is a small number and  $\ell$  is the beam radius.

We are exploring, as one possible coupling mechanism, the non-uniform plasma resonances discussed in the previous section. These resonances set up the high-order radial field variations required to excite transverse velocity beam waves. The resonances themselves may be excited by electrodes which are located entirely outside the beam-plasma region. (See Fig. 8.)

Many experiments related to this aspect have been conducted. From these experiments, it appears that the core resonances in a plasma are strongly excited by an external circuit. The depth of the absorption is well illustrated in Fig. 7, which shows oscilloscope traces of resonant dips in reflected power as viewed on a strip line excited at a frequency of 400 Mc/sec. Each trace is for the indicated ratio of wave frequency to cyclotron frequency;

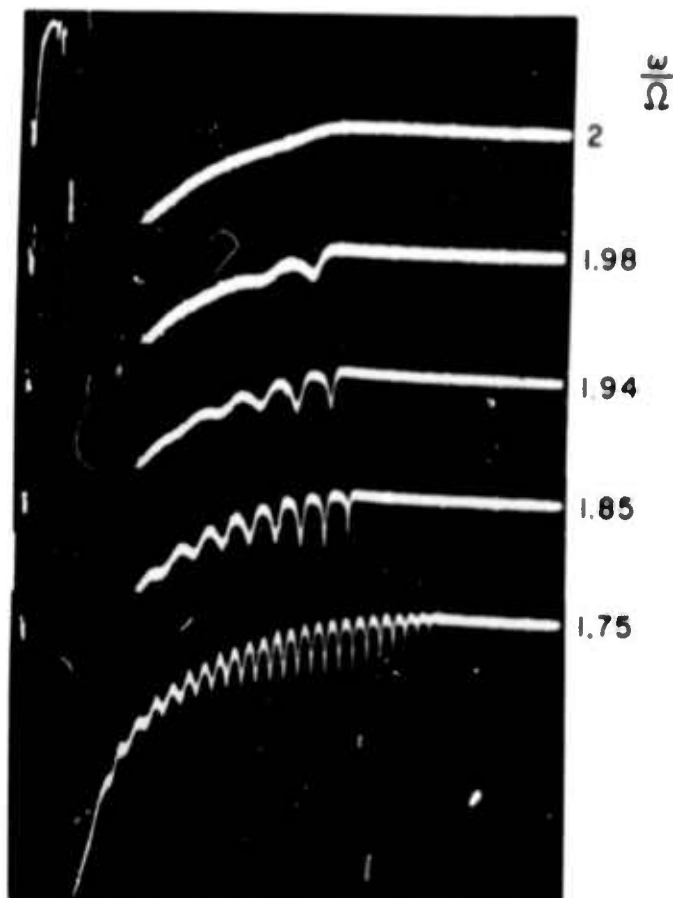


FIG. 7 Experimentally observed radial electron plasma wave resonances in the core of a cylindrical plasma column for different magnetic field strengths, observed in reflection in a neon afterglow plasma, 0.02 torr,  $f = 400$  Mc/sec, time scale 0.2 msec/div. Note depth of resonant structure.



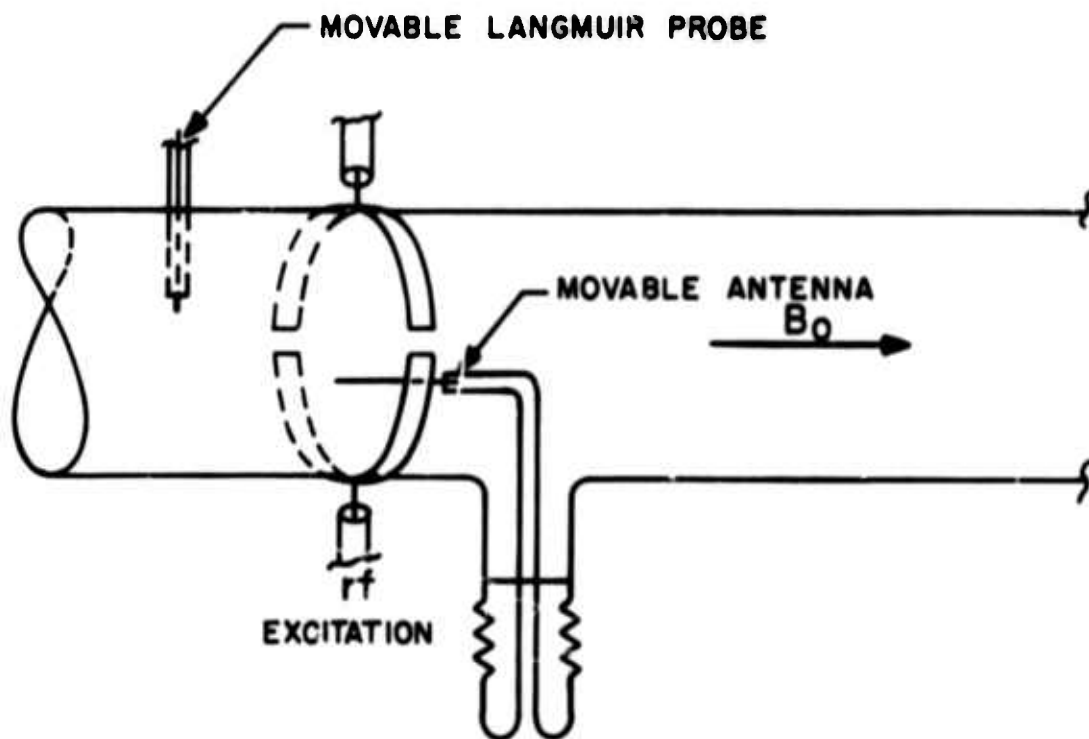


FIG. 8 Experimental apparatus showing method of excitation as well as method of internal probing of radial resonances on a plasma column in magnetic field. The rf excitation at 1175 Mc/sec is made on a capacitive type system employing striplines fed out of phase. A simple coaxial cable with the center conductor bared for one inch serves as the probe inside the dc discharge.

all traces are in the vicinity of the second harmonic of the cyclotron frequency, as predicted by the dispersion relation of Bernstein<sup>12</sup> from longitudinal waves propagating across the magnetic field.

#### IV. WORK PERFORMED DURING REPORT PERIOD

##### A. Theoretical

Electrostatic waves in a magnetized plasma propagating in directions perpendicular to the magnetic field are described by the Bernstein dispersion relation.<sup>12</sup> However, the Bernstein modes are for a Maxwellian plasma and do not allow for deviations from the perpendicular. The waves in a typical experiment probably have some component of wave number along the magnetic field, and in this context such oblique propagation is particularly desirable to facilitate coupling to external circuitry. Moreover, discharges may have some non-Maxwellian velocity distribution.

The Fourth Quarterly Report described the dispersion relation for Druyvestyn and exponential distribution functions and perpendicular propagation. The numerical results were reported in the Gruber and Bekefi paper included as an appendix to the Fifth Quarterly Report. The essential conclusion was that the dispersion relation was not significantly different for non-Maxwellian velocity distributions.

During this quarter, numerical results have been obtained for propagation in a Maxwellian plasma in directions slightly away from the perpendicular. This removes the other restriction to the Bernstein modes. Large deviations from the perpendicular rapidly lead to large damping. This is well known and is also evident from the numerical results.

The numerical work has been simplified by considering the case  $\omega_p \gg \Omega$ . The dispersion relation follows directly from Eq. (1) and is

$$1 + \frac{\omega}{\sqrt{2} k_{\parallel} v_T} \sum_{n=-\infty}^{\infty} e^{-\lambda_{\perp}} I_n(\lambda_{\perp}) Z(\alpha_n) = 0$$

where

$$v_T = \left( \frac{kT}{m} \right)^{1/2} = \text{thermal velocity}$$

$$\lambda_{\perp} = (k_{\perp} v_T / \Omega)^2$$

$$\lambda_{\parallel} = (k_{\parallel} v_T / \Omega)^2$$

$$\alpha_n = \frac{\omega - n\Omega}{\sqrt{2} k_{\parallel} v_T}$$

The  $I_n(\lambda_\perp)$  are modified Bessel functions and  $Z(\alpha_n)$  is the plasma dispersion function. Our interest is in frequencies where  $\omega \approx z\Omega$  and  $\lambda_\perp \lesssim 2.0$ . It is therefore sufficient to include only  $-10 \leq n \leq 10$ ; the relationship above can then be simplified to

$$\sum_{n=0}^{10} \left[ 2 - \frac{s}{s+n} + \frac{s}{\sqrt{2}\lambda_\parallel} Z(\alpha_n) I_n(\lambda_\perp) \right] = 0$$

where  $s = \omega/\Omega$ . Values of  $\lambda_\perp$  that satisfy this relation for real values of  $s$  and  $\lambda_\parallel$  have been obtained. The  $Z$  function is complex, which requires that  $\lambda_\perp$  be complex.

Solutions for  $\lambda_\parallel \leq 0.20$  are shown in Figs. 9 and 10. The value of  $\lambda_\parallel = 0.10$  corresponds to an axial wavenumber,  $k_\parallel$ , of about 5.0 and an axial wavelength of about 1.3 cm. The curves labeled  $\lambda_\parallel = 0$  are the Bernstein modes in the high density limit ( $\omega_p \gg \Omega$ ). The  $\lambda_\parallel > 0$  curves all go into  $s=0$  for  $\text{Re}\sqrt{\lambda_\perp} = 0$ . The points are experimental values obtained recently (see next section). The experimental parameters are not sufficiently well known to determine  $\text{Im}\sqrt{\lambda_\perp}$  by this comparison, but a value of  $\text{Im}\sqrt{\lambda_\perp} < 0.01$  is required for propagation without unreasonable damping.

## B. Modulated Beam Experiment

### 1. Beam Excitation of Longitudinal Waves

The observation of longitudinal waves excited with the modulated beam, described in the last report, required the use of magnetic field modulation and a phase-sensitive detection technique. We have recently observed more efficient excitation of the waves and have been able to detect them with an ordinary superheterodyne receiver. At the same time, we have found a dependence of excitation efficiency on the transverse energy of the beam electrons.

Figure 11 shows the intensity of the signal picked up by a probe which was moved radially across a mercury discharge without magnetic field modulation or phase sensitive detection. As before, it has been assumed that the observed intensity variation is due to a beat between a traveling longitudinal wave in the plasma and a very long wavelength oscillation at the same frequency. The radial wavelength (the separation between peaks in Fig. 11) was measured as a function of magnetic field and compared with the theoretical calculations in Fig. 9. It is not known why previous measurements of the radial wavelength (see Fig. 16 of the Fifth Quarterly Report) disagree with the theory, although some of the parameters which affect the excitation efficiency may also affect the dispersion of the waves. In order to plot the experimental points in Fig. 9, where  $\sqrt{\lambda} = k_\perp v_T / \Omega$ ,  $v_T$  was taken to be  $9.1 \times 10^7$  cm/sec, corresponding to a 4.7 eV electron temperature. This value was obtained previously from Langmuir probe measurements.

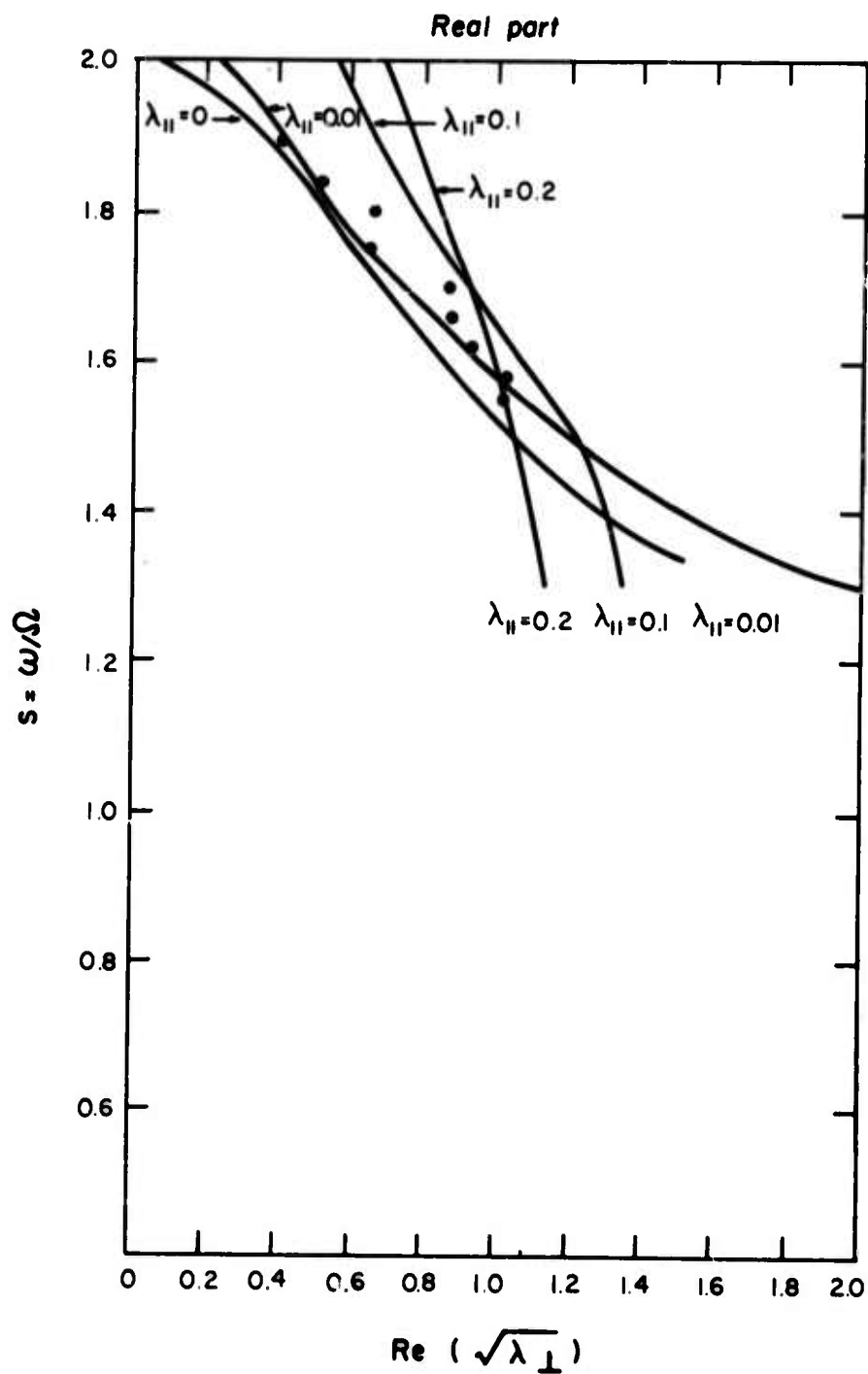


FIG. 9 The real part of  $\sqrt{\lambda_{\perp}}$  vs  $\omega/\Omega$  for a range of  $\lambda_{\parallel}$ . The Bernstein modes are  $\lambda_{\parallel} = 0$ . The curves for  $\lambda_{\parallel} > 0$  eventually bend into the origin. The dots are experimental points (see Sec. B).

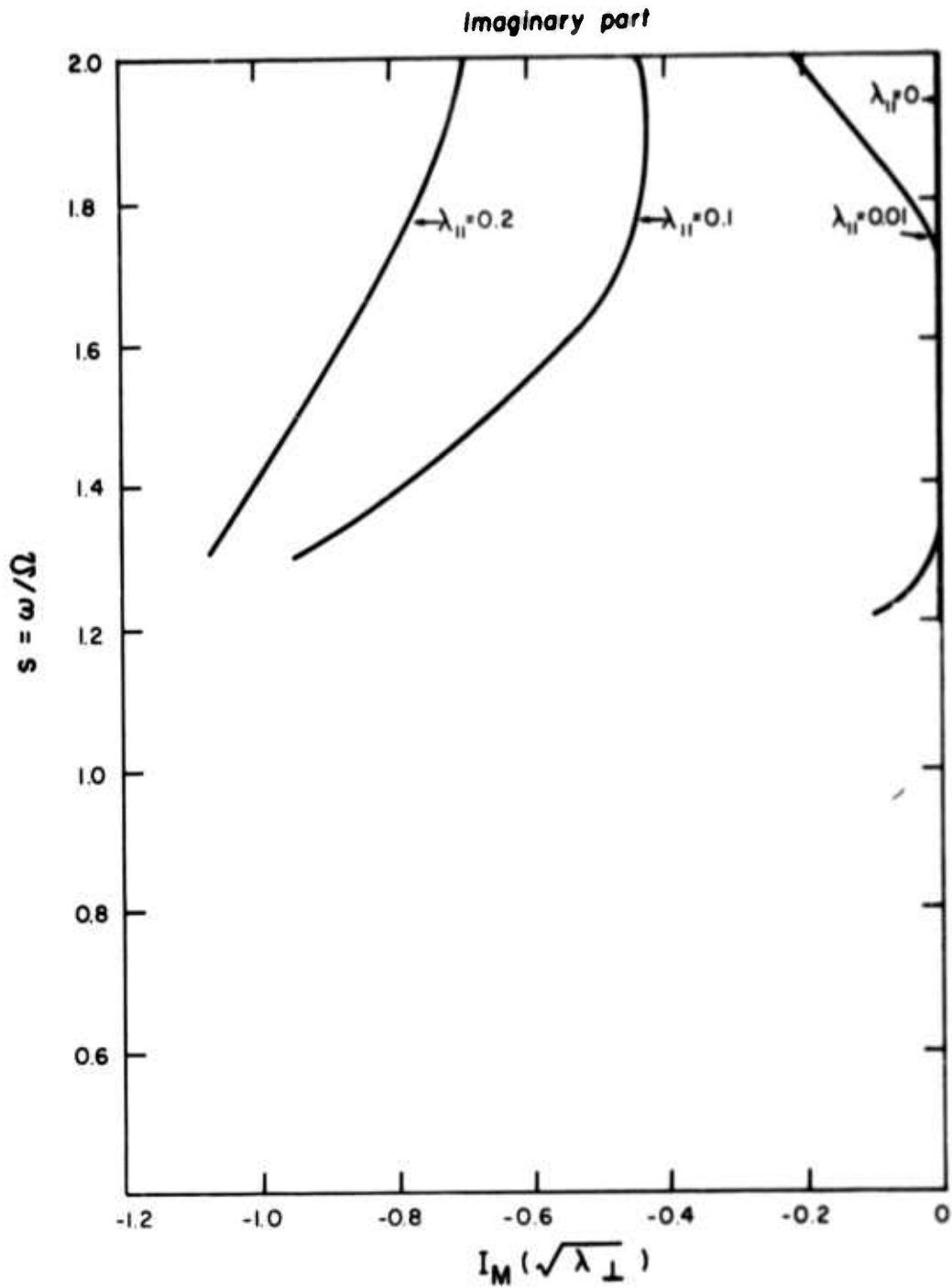


FIG. 10 The imaginary part of  $\sqrt{\lambda_\perp}$  vs  $\omega/\Omega$  for a range of  $\lambda_\parallel$ . The Bernstein modes are  $\lambda_\parallel = 0$  and have zero imaginary part (no damping). The  $I_M/\lambda_\perp$  must be  $< 0.01$  for reasonable damping.

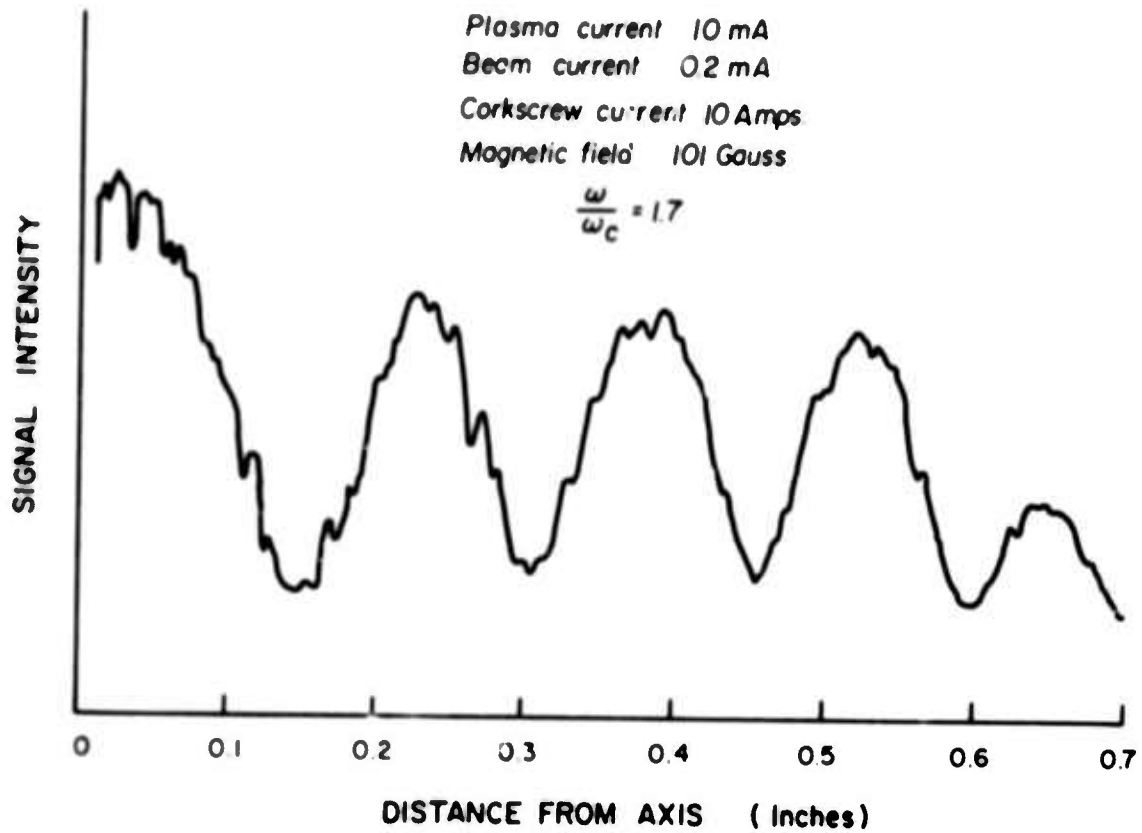


FIG. 11 The intensity of the probe signal as a function of its radial position without magnetic-field modulation or phase-sensitive detection.

The variation of signal intensity with corkscrew current is shown in Figs. 12 and 13. The intensity was measured at each of four peaks observed when the probe was moved radially outwards as in Fig. 11. The first and third peaks were of somewhat greater intensity than the second and fourth peaks (the first peak was the one closest to the axis of the beam). For these peaks the intensity increases approximately exponentially with the corkscrew current. If the helix is operating according to theoretical predictions, the transverse velocity of the electrons in the beam is proportional to the corkscrew current. The reason for the reduction in signal intensity with corkscrew current about 10 A is not understood, unless the increase in diameter of the beam with transverse velocity causes the beam to impinge on some limiting aperture in the system.

## 2. Axial Measurements

An antenna which could be moved in an axial direction was incorporated in the modulated-beam experiment. The purpose of the antenna was to detect growth in the system and to try to measure the axial wavelength of the longitudinal waves. No significant change in the intensity of the spectrum was observed as the antenna was moved to different axial positions. However, the antenna could be moved only over a distance of about eight inches close to the cathode of the main discharge. The region where the transverse energy beam enters the plasma, where growth is more likely to occur without the signal reaching a saturation level, could not be probed. The apparatus is being modified to allow growth measurements in this region.

No measurements of the axial wavelength were obtained because of the difficulty of accurately moving the antenna parallel to the electron beam. This is a necessary requirement because of the small radial wavelength ( $\sim 1$  mm): Large changes in phase with axial position can arise from slight variations in radial position as the antenna is moved.

In order to overcome this problem, measurements were made with the antenna fixed while the axial properties of the system were changed by altering the electron beam voltage. As the voltage was varied, the phase of the antenna signal also varied, a result mentioned in the previous report. Figure 14 shows the antenna signal as a function of the beam voltages obtained with field modulation and phase-sensitive detection. If the phase variations were due to the existence of an axial wavelength equal to the separation between charge maxima on the beam, the phase variations should be independent of magnetic field. This is not the case (see Fig. 14). Furthermore, the theoretical calculations described in Sec. A above indicate that strong damping of the longitudinal waves would occur with an axial wavelength of this magnitude ( $\sim 1$  cm).

## C. Two-Beam Experiment

We have restarted work on an experiment to study the interaction of two interpenetrating electron beams, one with an appreciable amount of transverse energy, in an axial magnetic field. At the same time, we are investigating methods of measuring the transverse energy on an electron beam. The flexibility and size of the two-beam facility make it very suitable for this sort of measurement.

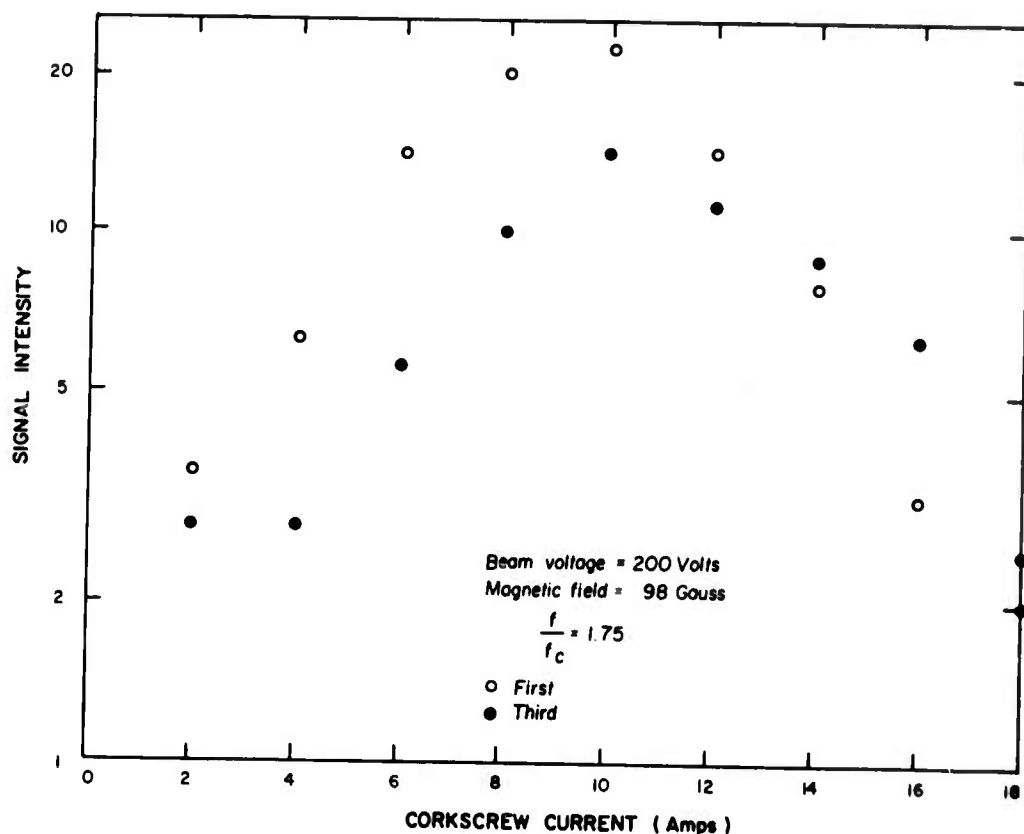


FIG. 12 The intensity of the signal at the first and third radial peaks as a function of corkscrew current.

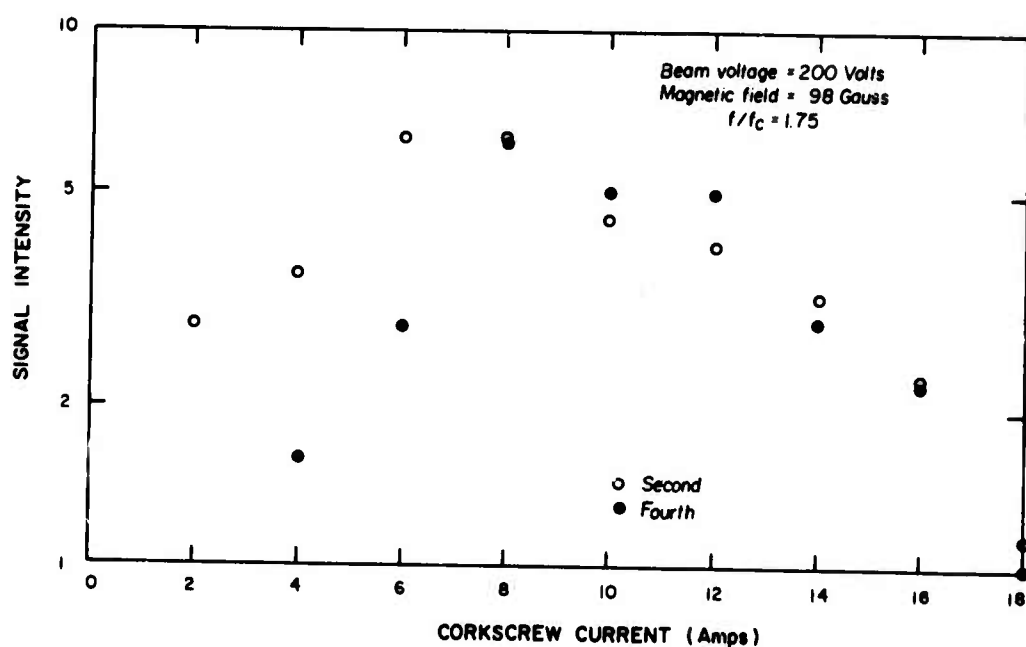


FIG. 13 The intensity of the signal (same units as in Fig. 12) at the second and fourth radial peaks as a function of corkscrew current.



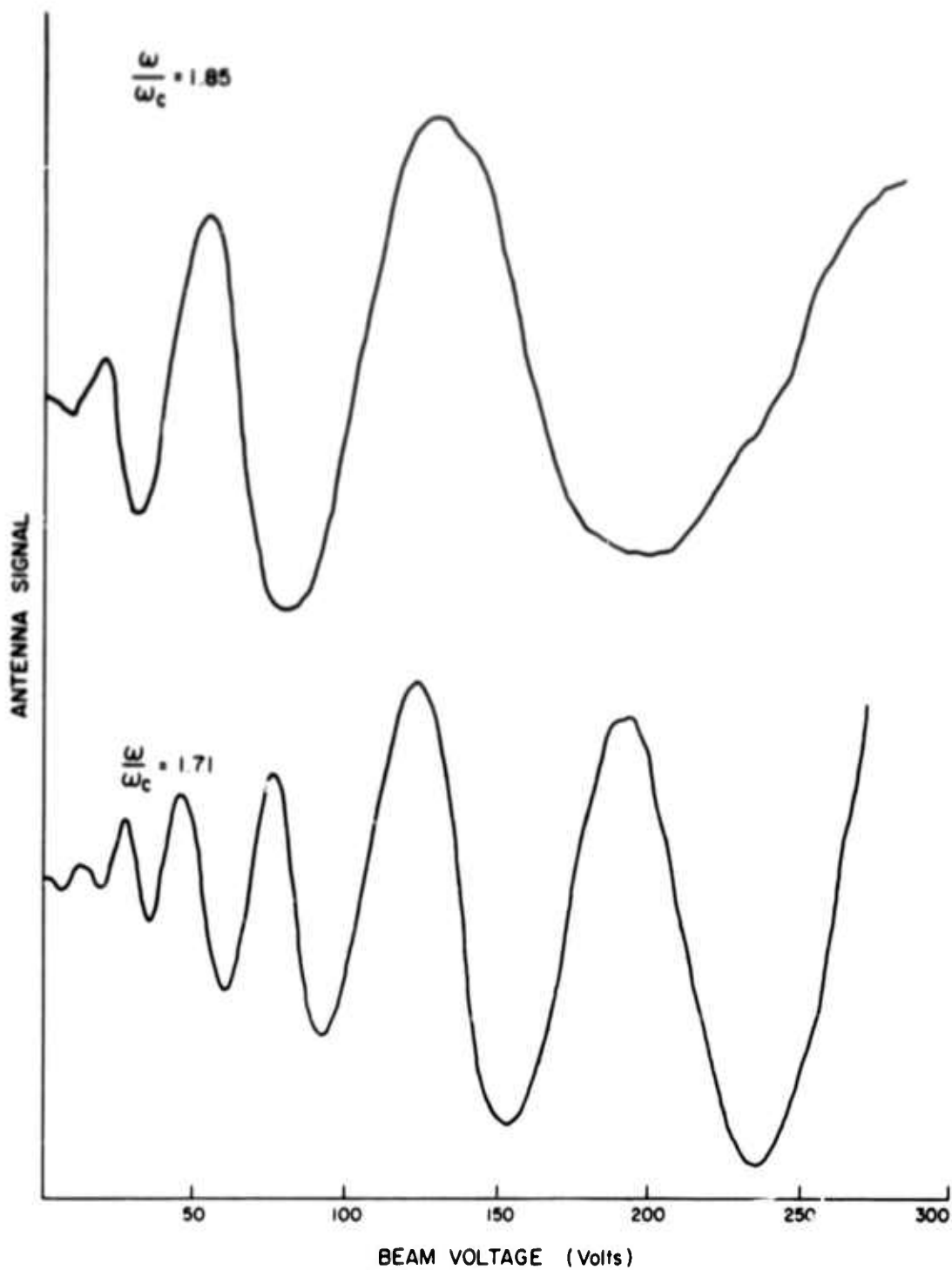


FIG. 14 Phase variation of the signal with the antenna fixed as a function of beam voltage for two magnetic fields.

A beam with transverse energy may be obtained from one with only axial motion by the use of a helical ("corkscrew") magnetic field of variable pitch.<sup>13,14</sup> The field configuration consists of the uniform axial field superimposed upon a transverse perturbing field which rotates spatially in phase with a particle in resonance. This method has been used to provide transverse energy in the beam plasma and modulated beam experiments (see previous section). However, it has the disadvantage that the required perturbing field is unique with respect to the total beam energy and the steady axial magnetic field. An adjustment of either of these quantities requires a new design for the helical perturbing field. An alternative method for obtaining appreciable transverse energy is to aim the beam into a region of increasing magnetic field at an angle with respect to the symmetry axis. Since the magnetic moment is a constant of the motion, the initial transverse energy is increased in direct proportion to the increasing field. The axially directed energy is reduced correspondingly.

During this quarter, several experiments were carried out to obtain an indication of the transverse energy imparted to an electron beam by the methods described above. In the first of these experiments a probe was used to measure the azimuthal flux ( $\Gamma_{\perp}$ ) in an electron beam which had passed through a helical perturbing field. The experimental arrangement is shown in Fig. 15. The probe had two exposed metallic surfaces which faced in opposite directions and which were oriented perpendicular to the azimuthal direction (the r-z plane of a cylindrical coordinate system). With zero helix current, the outputs from the probe were balanced for a null indication. A typical plot of the output potential  $\phi(\propto \Gamma_{\perp})$  vs helix current is shown in Fig. 16 for a magnetic field of 80 gauss and a beam energy of 200 eV. Although no absolute measure of the transverse energy has been obtained from this preliminary experiment, it is evident that there is an increase in the transverse flux as the perturbing field is increased.

Another method of determining the transverse energy is to measure the magnetic field associated with the diamagnetism of an electron beam. The change in the axial magnetic field due to the transverse motion is

$$\delta B_z = \mu_0 e \int_0^R \Gamma_{\perp} dr$$

where  $\Gamma_{\perp}$  is the azimuthal flux and the integration is with respect to radial distance from the beam center.

An experiment has been performed which used the above effect as an indication of transverse energy. A 200 eV electron beam was modulated at 1000 Hz. The gun was aimed into a region of increasing magnetic field at the end of a uniform solenoid at an angle of  $30^\circ$  with respect to the axis. A 2000 turn,  $1\frac{1}{2}$  inch inside diameter electrostatically shielded pickup coil was placed coaxially within, and well inside, the solenoid where the magnetic field was uniform. Signals received from a small, known azimuthal current indicated a sensitivity to axial magnetic field fluctuations on the order

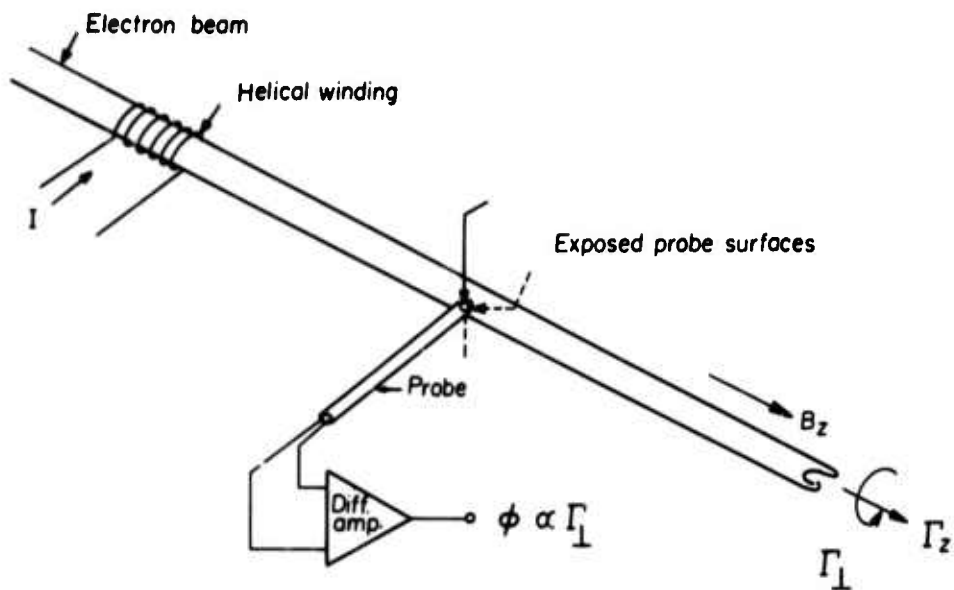


FIG. 15 Experimental setup for measuring the azimuthal flux on an electron beam with a probe with two exposed surfaces.

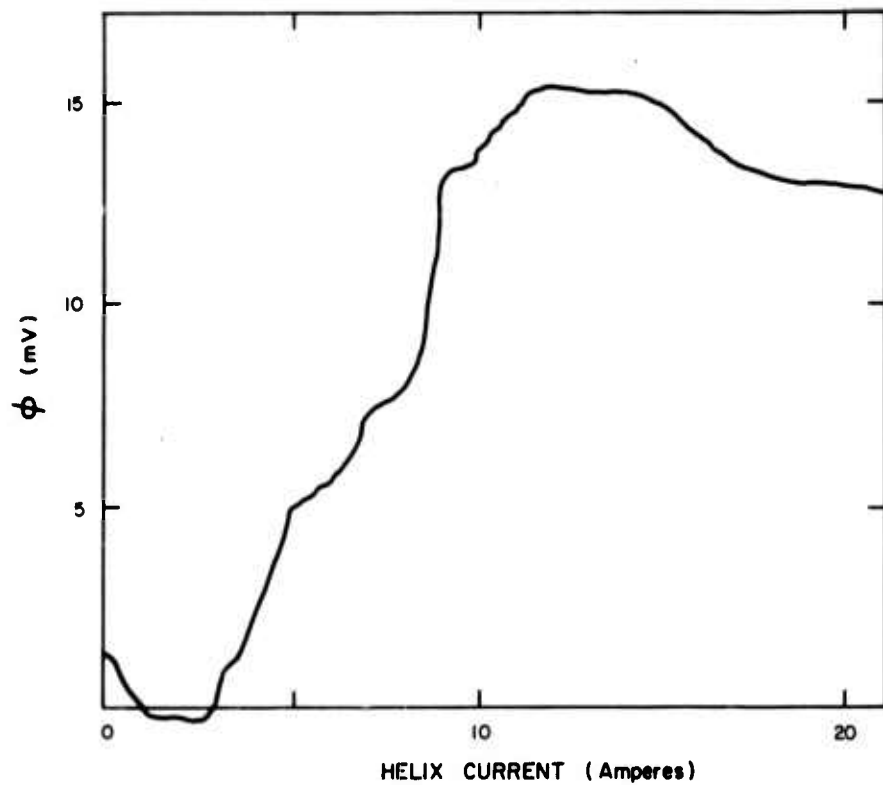


FIG. 16 Differential probe output as a function of helix current.

of 50 milligauss. With the beam turned on, large signals at the modulation frequency were observed, indicating the presence of appreciable transverse energy.

#### V. CONCLUSIONS

As the transverse energy of the beam is increased, longitudinal plasma waves are excited more efficiently by a modulated electron beam. Calculations of the damping of the waves for oblique propagation show that the axial wavelength must be larger than the separation of charge maxima in the electron beam.

#### VI. FUTURE PLANS

Growth measurements will be made in the region where the modulated beam enters the plasma. Further experiments are planned to obtain an absolute measure of the transverse energy imparted to the beam by the corkscrew field and when the beam is injected at an angle to the magnetic field. The radiation from a transverse energy beam and from a transverse energy beam interacting with an axial beam will also be studied.

#### LITERATURE CITED

1. R. W. Gould and A. W. Trivelpiece, A New Mode of Wave Propagation on Electron Beams, Proceedings of the Symposium on Electronic Waveguides, (Polytechnic Press, Brooklyn, New York, 1958).
2. L. D. Smullin and P. Chorney, Propagation in Ion Loaded Waveguides, ibid.
3. P. L. Auer and S. Gruber, Bull. Am. Phys. Soc. II 9, 565 (1964).
4. S. Gruber, Bull. Am. Phys. Soc. II 10, 221 (1965).
5. A. Bers and S. Gruber, Appl. Phys. Letters 6, 27 (1965).
6. S. Gruber, M. W. Klein and P. L. Auer, Phys. Fluids 8, 1504 (1965).
7. A. Simon and M. N. Rosenbluth, Phys. Fluids 6, 1566 (1963).
8. J. Nickel, J. Parker and R. W. Gould, Phys. Fluids 7, 1489 (1964).
9. S. J. Buchsbaum and A. Hasegawa, Phys. Rev. Letters 12, 685 (1964).
10. H. J. Schmitt, G. Meltz and P. J. Freyheit, Phys. Rev. 139, A1432 (1965).
11. K. Mitani, H. Kubo and S. Tanaka, J. Phys. Soc. (Japan) 19, 221 (1964).
12. J. B. Bernstein, Phys. Rev. 109, 10 (1958).
13. R. C. Wingerson, T. H. Dupree and D. J. Rose, Phys. Fluids 7, 1475 (1964).
14. L. M. Lidsky, Phys. Fluids 7, 1484 (1964).

## Security Classification

## DOCUMENT CONTROL DATA - R&amp;D

(Security classification of title, body of abstract and indexing annotation must be entered when the overall report is classified)

1. ORIGINATING ACTIVITY (Corporate author)  SPERRY RAND RESEARCH CENTER SUDBURY, MASSACHUSETTS 01776		2a. REPORT SECURITY CLASSIFICATION  unclassified	
		2b. GROUP  ---	
3. REPORT TITLE  INVESTIGATION OF HIGH-POWER BEAM-PLASMA INTERACTIONS			
4. DESCRIPTIVE NOTES (Type of report and inclusive dates)  Sixth Quarterly Report: 15 March 1967 - 14 June 1967			
5. AUTHOR(S) (Last name, first name, initial)  Lustig, Claude; Stone, Philip M.; Ewald, Harry			
6. REPORT DATE  September 1967		7a. TOTAL NO. OF PAGES  38	7b. NO. OF REFS  14
8a. CONTRACT OR GRANT NO.  DA 28-043-AMC-01821(E)		9a. ORIGINATOR'S REPORT NUMBER(S)  SRRC-CR-67-39	
a. PROJECT NO.  7900.21.243.40.01			
c. ARPA Order No. 695		9b. OTHER REPORT NO(S) (Any other numbers that may be assigned this report)  LCON-01821-6	
10. AVAILABILITY/LIMITATION NOTICES Each transmittal of this document outside the Department of Defense must have prior approval of CGO, U. S. Army Electronics Command, Fort Monmouth, N. J. Attn: AMSEL-KL-TG			
11. SUPPLEMENTARY NOTES  Advanced Research Projects Agency ARPA Order No. 695		12. SPONSORING MILITARY ACTIVITY  U. S. Army Electronics Command Fort Monmouth, N. J. 07703 Attn: AMSEL-KL-TG	
13. ABSTRACT This research is directed toward the investigation of high-power beam plasma interactions, with specific investigation of the transverse velocity beam modes called for.  The dispersion relation for electrostatic waves propagating at an oblique angle to the magnetic field has been calculated. Strong damping occurs unless the axial wavelength is at least one or two orders of magnitude greater than the perpendicular wavelength. In experiments with the modulated-beam apparatus, we have found that the electrostatic waves are excited more strongly as the transverse energy of the beam is increased. Experiments are being carried out to obtain a quantitative measure of the transverse energy of an electron beam.  This research is part of PROJECT DEFENDER, sponsored by the Advanced Research Project Agency, Department of Defense, and administered by the U. S. Army Electronics Command under Contract No. DA 28-043-AMC-01821(E).			

DD FORM 1473

Security Classification

14

## KEY WORDS

Beam-plasma interactions  
Microwave devices  
Electron beams  
Electrostatic wave resonance  
Plasma column resonance  
Wave coupling

## LINK A

## LINK B

## LINK C

ROLE

WT

ROLE

WT

ROLE

WT

## INSTRUCTIONS

1. **ORIGINATING ACTIVITY:** Enter the name and address of the contractor, subcontractor, grantee, Department of Defense activity or other organization (corporate author) issuing the report.

2a. **REPORT SECURITY CLASSIFICATION:** Enter the overall security classification of the report. Indicate whether "Restricted Data" is included. Marking is to be in accordance with appropriate security regulations.

2b. **GROUP:** Automatic downgrading is specified in DoD Directive 5200.10 and Armed Forces Industrial Manual. Enter the group number. Also, when applicable, show that optional markings have been used for Group 3 and Group 4 as authorized.

3. **REPORT TITLE:** Enter the complete report title in all capital letters. Titles in all cases should be unclassified. If a meaningful title cannot be selected without classification, show title classification in all capitals in parenthesis immediately following the title.

4. **DESCRIPTIVE NOTES:** If appropriate, enter the type of report, e.g., interim, progress, summary, annual, or final. Give the inclusive dates when a specific reporting period is covered.

5. **AUTHOR(S):** Enter the name(s) of author(s) as shown on or in the report. Enter last name, first name, middle initial. If military, show rank and branch of service. The name of the principal author is an absolute minimum requirement.

6. **REPORT DATE:** Enter the date of the report as day, month, year, or month, year. If more than one date appears on the report, use date of publication.

7a. **TOTAL NUMBER OF PAGES:** The total page count should follow normal pagination procedures, i.e., enter the number of pages containing information.

7b. **NUMBER OF REFERENCES:** Enter the total number of references cited in the report.

8a. **CONTRACT OR GRANT NUMBER:** If appropriate, enter the applicable number of the contract or grant under which the report was written.

8b, 8c, & 8d. **PROJECT NUMBER:** Enter the appropriate military department identification, such as project number, subproject number, system numbers, task number, etc.

9a. **ORIGINATOR'S REPORT NUMBER(S):** Enter the official report number by which the document will be identified and controlled by the originating activity. This number must be unique to this report.

9b. **OTHER REPORT NUMBER(S):** If the report has been assigned any other report numbers (either by the originator or by the sponsor), also enter this number(s).

10. **AVAILABILITY/LIMITATION NOTICES:** Enter any limitations on further dissemination of the report, other than those

imposed by security classification, using standard statements such as:

- (1) "Qualified requesters may obtain copies of this report from DDC."
- (2) "Foreign announcement and dissemination of this report by DDC is not authorized."
- (3) "U. S. Government agencies may obtain copies of this report directly from DDC. Other qualified DDC users shall request through \_\_\_\_\_."
- (4) "U. S. military agencies may obtain copies of this report directly from DDC. Other qualified users shall request through \_\_\_\_\_."
- (5) "All distribution of this report is controlled. Qualified DDC users shall request through \_\_\_\_\_."

If the report has been furnished to the Office of Technical Services, Department of Commerce, for sale to the public, indicate this fact and enter the price, if known.

11. **SUPPLEMENTARY NOTES:** Use for additional explanatory notes.

12. **SPONSORING MILITARY ACTIVITY:** Enter the name of the departmental project office or laboratory sponsoring (paying for) the research and development. Include address.

13. **ABSTRACT:** Enter an abstract giving a brief and factual summary of the document indicative of the report, even though it may also appear elsewhere in the body of the technical report. If additional space is required, a continuation sheet shall be attached.

It is highly desirable that the abstract of classified reports be unclassified. Each paragraph of the abstract shall end with an indication of the military security classification of the information in the paragraph, represented as (TS), (S), (C), or (U).

There is no limitation on the length of the abstract. However, the suggested length is from 150 to 225 words.

14. **KEY WORDS:** Key words are technically meaningful terms or short phrases that characterize a report and may be used as index entries for cataloging the report. Key words must be selected so that no security classification is required. Identifiers, such as equipment model designation, trade name, military project code name, geographic location, may be used as key words but will be followed by an indication of technical context. The assignment of links, rules, and weights is optional.